medicina

MDPI

Article

A Pilot Experiment to Measure the Initial Mechanical Stability of the Femoral Head Implant in a Cadaveric Model of Osteonecrosis of Femoral Head Involving up to 50% of the Remaining Femoral Head

Seungha Woo, Youngho Lee and Doohoon Sun *

Department of Orthopedic Surgery, Daejeon Sun Hospital, 29 Mokjung-ro, Jung-gu, Daejeon 34811, Republic of Korea
* Correspondence: sunosdoctor@gmail.com; Tel.: +82-422-208-460; Fax: +82-422-208-464

Abstract: *Background and Objectives:* Currently, only patients with osteonecrosis of the femoral head (ONFH), who had bone defects involving 30–33.3% of the remaining femoral head, are indicated in hip resurfacing arthroplasty (HRA). In an experimental cadaver model of ONFH involving up to 50% of the remaining femoral head, the initial stability of the femoral head implant (FHI) at the interface between the implant and the remaining femoral head was measured. *Materials and Methods:* The ten specimens and the remaining ten served as the experimental group and the control group, respectively. We examined the degree of the displacement of the FHI, the bonding strength between the FHI and the retained bone and that at the interface between the FHI and bone cement. *Results:* Changes in the degree of displacement at the final phase from the initial phase were calculated as 0.089 ± 0.036 mm in the experimental group and 0.083 ± 0.056 mm in the control group. However, this difference reached no statistical significance ($p = 0.7789$). Overall, there was an increase in the degree of displacement due to the loading stress, with increased loading cycles in both groups. In cycles of up to 6000 times, there was a steep increase. After cycles of 8000 times, however, there was a gradual increase. Moreover, in cycles of up to 8000 times, there was an increase in the difference in the degree of displacement due to the loading stress between the two groups. After cycles of 8000 times, however, such difference remained almost unchanged. *Conclusions:* In conclusion, orthopedic surgeons could consider performing the HRA in patients with ONFH where the bone defects involved up to 50% of the remaining femoral head, without involving the femoral head–neck junction in the anterior and superior area of the femoral head. However, more evidence-based studies are warranted to justify our results.

Keywords: bone defect; femoral head; osteonecrosis of femoral head; resurfacing arthroplasty; stability

Citation: Woo, S.; Lee, Y.; Sun, D. A Pilot Experiment to Measure the Initial Mechanical Stability of the Femoral Head Implant in a Cadaveric Model of Osteonecrosis of Femoral Head Involving up to 50% of the Remaining Femoral Head. *Medicina* **2023**, *59*, 508. https://doi.org/10.3390/medicina59030508

Academic Editor: Woo Jong Kim

Received: 3 January 2023
Revised: 27 February 2023
Accepted: 1 March 2023
Published: 5 March 2023

1. Introduction

Osteonecrosis of the femoral head (ONFH), also referred to as avascular necrosis, is defined as a pathologic condition arising from an ischemic injury that is characterized by both a crucial disruption of blood supply to the bone and an increase in the intraosseous pressure. Subsequently, this results in the degradation of the organic elements of the bone and the marrow, thus commonly leading to a collapse of subchondral bone in the femoral head [1–4]. As such, ONFH is a debilitating, progressive joint disease of idiopathic origin; it is an interesting topic from both clinical and economic perspectives [5–7]. Over the past few years, there has been an increase in the prevalence of ONFH [8]. Moreover, it has been diagnosed with increasing frequency in young adults and has a significant socioeconomic impact [9]. The annual number of patients who are hospitalized for the treatment of ONFH is estimated at 10,000–20,000 in the US [5]. It is a serious disease entity that may affect the quality of life in patients with ONFH [10]. Still, however, little is known about the

risk factors associated with its pathogenesis and pathophysiology, although they include the long-term use of chronic steroids, smoking, alcoholism, hip trauma and prior hip surgery [11,12]. This makes it difficult to define surgical methods and curative effects [1,13]. It is, therefore, crucial to obtain a better understanding of the pathogenesis of and make therapeutic approaches to ONFH [8]. Despite recent advancements in diagnostic modalities, effective treatments have been elusive and a majority of cases of ONFH eventually result in a collapse of the femoral head. Most of the surgical modalities for patients with ONFH aim to prevent the collapse of the subchondral bone, although their clinical outcomes have been reported to be inconsistent [1,13]. Core decompression may be effective for the treatment of early-stage ONFH, although femoral osteotomy, vascularized or non-vascularized bone grafting and total hip arthroplasty (THA) may also be attempted for that of advanced ONFH [14].

Patients with ONFH account for 5–12% of those undergoing THA in the US [1]. If treated conservatively, >80% of affected hips would progress to femoral collapse and the destruction of the hip joint within four years of initial diagnosis; this often requires THA [15]. In the early stage of ONFH, joint-preserving surgical techniques are often considered. However, this causes problems, such as a significant failure rate and morbidity [16–19]. THA is often a mainstay of treatment in patients with osteonecrosis of the hip [18]. However, it may be not an attractive treatment option for younger patients; it would be desirable to avoid or delay THA. This is not only because most of the younger patients would outlive the current state-of-the art implants, but also because it has been suggested that such patients are less satisfied with its clinical outcomes [17,20]. It is therefore imperative that effective treatment modalities be developed, which would be essential for preventing the collapse of affected femoral heads or prolonging the interval between initial diagnosis and THA [7]. To date, diverse small animal models using rats or rabbits have been used to develop new treatment modalities for ONFH. Thus, these animal models induce ONFH by systematic insult, including steroid administration or steroid combined with another adjunct agent [21–27]. It would also be mandatory, however, to improve the relevance of animal models of ONFH in a clinical setting.

Both hemi-resurfacing arthroplasty and metal-on-metal hip resurfacing arthroplasty (HRA) are alternatives to conventional THA for patients with ONFH [28–30]. Hemi-resurfacing and total resurfacing arthroplasty are referred to as the prosthetic replacement of the femoral side only and that of both the femoral head and the acetabular surface, respectively [31]. According to a US nationwide study, the frequency of THA was the highest (90%), followed by HRA (0.2%) and osteotomy (1%) [32]. Both hemi-resurfacing arthroplasty and HRA are potentially advantageous in preserving bone and the loading of the proximal femur, lowering a risk of dislocation and eliminating the polyethylene debris that may cause osteolysis as compared with conventional THA [30,33,34]. Consequently, HRA is considered an appropriate option for young and active patients with ONFH [35].

However, there are things to consider regarding the indications of HRA in the context of regulatory requirements enforced by the US Food and Drug Administration (FDA). In 2006, the US FDA approved the clinical use of a metal-on-metal (MoM) resurfacing implant for primary HRA. This is based on the pre-market approval (PMA) process in 2385 patients with non-inflammatory or inflammatory arthritis receiving the Birmingham Hip Resurfacing (BHR) System (Smith & Nephew Orthopaedics, Memphis, TN) [36,37]. Later, in 2007 and 2009, the US FDA approved the clinical use of two additional MoM resurfacing implants, such as the Cormet™ Hip Resurfacing System (Corin, Tampa, FL, USA) and the Conserve® Plus Total Hip Resurfacing System (MicroPort Orthopedics, Boston, MA, USA), respectively, in patients with non-inflammatory degenerative or inflammatory arthritis [38,39]. Since then, the US FDA has cleared a variety of implants for marketing through the 510(k) process [40]. According to the US FDA, however, patients with ONFH who had a necrotic area involving >50% of the femoral head are contraindicated in the use of MoM implants [41].

Given the above background, we created an experimental cadaver model of ONFH involving 50% of the remaining femoral head. We conducted this study to measure the initial stability of the FHI at the interface between the implant and the remaining femoral head.

2. Materials and Methods

2.1. Experimental Materials and Setting

We conducted the current biomechanical study using ten pairs of specimens from ten cadavers (n = 10). The specimens were preserved in a frozen state (−20 °C), and were gradually defrosted at room temperature for 24 h. A total of 20 specimens were equally divided into the experimental group (n = 10) and the control group (n = 10).

Inclusion criteria for the current experiment were a lack of pathologic bone lesions and the Singh index > 5. The Singh index is a typical classification system for the bone density of the femoral neck based on the qualitative visibility of the trabecular patterns [42].

The experimental procedures are schematically shown in Figure 1.

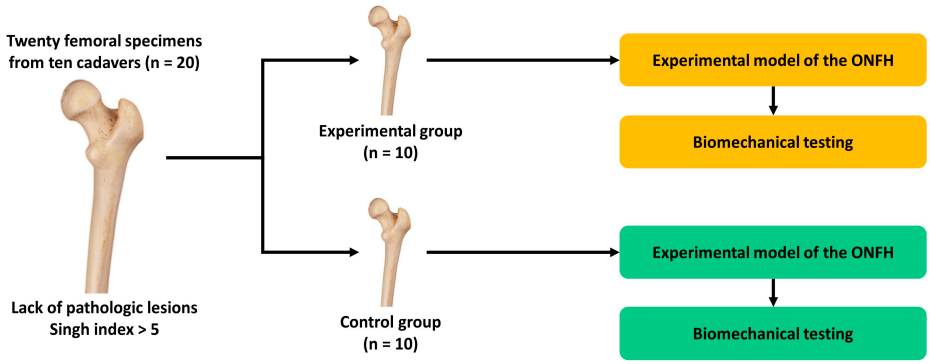

Figure 1. Experimental schema. Abbreviation: ONFH, osteonecrosis of femoral head.

2.2. Creation of an Experimental Model of ONFH

With a free-hand technique at an angle of 135° to the axis of the femoral shaft on the anterior–posterior plane and in parallel with the central axis of the femoral neck, we placed the femoral guide pin on the lateral plane. This was followed by the femoral reaming using a cannulated sleeve and a chamfering reamer with an appropriate size. After saline irrigation, we confirmed a lack of notching and inappropriate exposure of the cancellous bone at the femoral head–neck junction. Then, we dissected 50% of the antero-superior area of the remaining femoral head, and thereby caused bone defects in the experimental group. To consistently make bone defects, we mapped the area in dissecting the area of the femoral head (Figure 2).

Then, we placed an MoM implant (Durom®; Zimmer Inc., Warsaw, IN, USA) in the bone defect area and then fixed it using low-viscosity bone cement (Surgical Simplex® P; Stryker Howmedica Osteonics Corp., Rutherford, NJ, USA) for both groups. In the experimental group, however, we performed the same maneuver after restoring the bone defect area using a sufficient amount of low-viscosity bone cement.

2.3. Assessment of the Biomechanical Stability of the Specimen

We transected the specimen at the isthmus and then fixed it using a resin fixative (Vertex Self-Curing; Vertex-Dental B.V., Soesterberg, The Netherlands) (Figure 3A). We placed it on the machine at a valgus angle of 30°, thus attempting to preventing the fracture of the femoral neck while repeatedly applying a mechanical load to it.

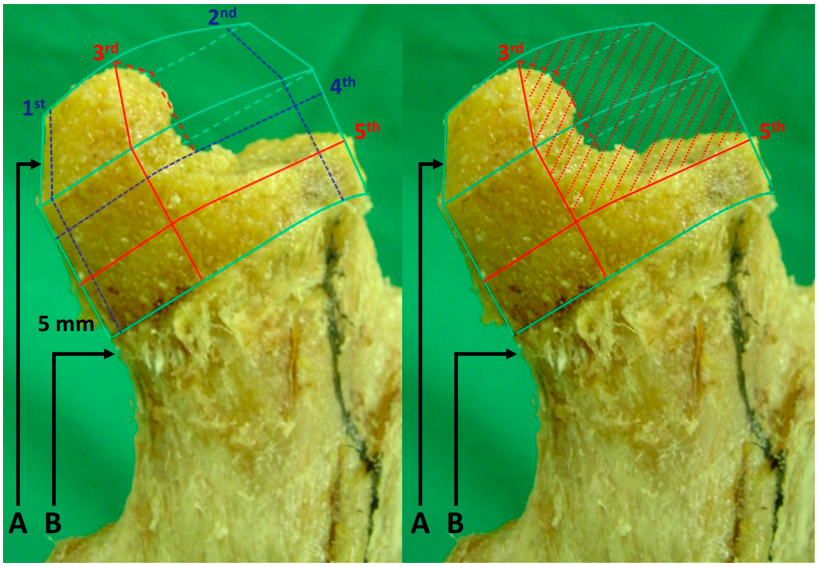

Figure 2. Anatomic specimens of the femur obtained from ten cadavers. Note: A: Femoral head, B: Femoral neck. We drew the 1st and 2nd lines along the midline of the femoral neck on the anterior–posterior and lateral plane, respectively. Then, we drew the 3rd line that crosses the 1st and 2nd lines from postero-superior to infero-anterior directions. We also drew the 4th line, that was vertical to the 3rd line and then crossed the center of the femoral head. In parallel with the 4th line, we drew the 5th line at 5 mm proximal to the head–neck junction. Finally, we dissected 50% of the antero-superior part of the remaining femoral head based on the 3rd and 5th lines.

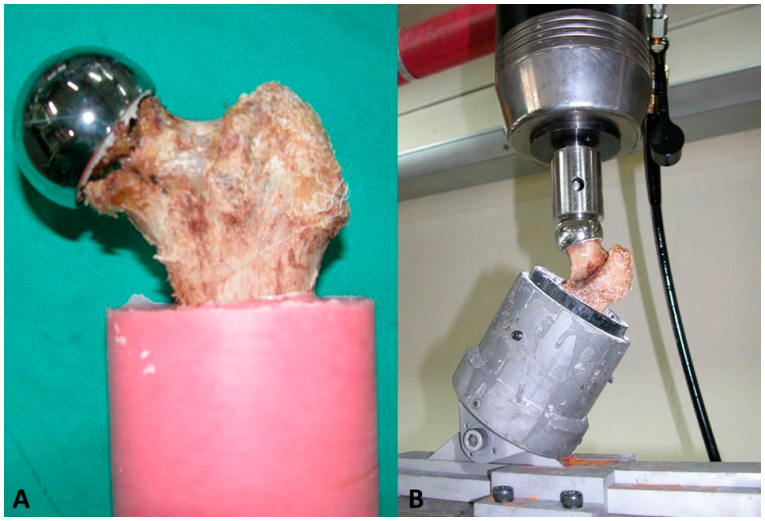

Figure 3. The preparation of the femoral specimens. (**A**) The femoral specimen was inserted in the resin block along the anatomical axis. (**B**) The femoral specimen with the femoral head implant was placed in a custom-made jig for the loading–unloading test.

We measured the biomechanical stability of the specimen using the dynamic testing machine based on the biaxial fluid pressure (Instron 8500®; Instron Corp., Norwood, MA, USA), for which we repeatedly applied a loading stress at a constant rate of 2 Hz [43,44]. The magnitude of loading stress ranged between 60 and 300 kg; it was five times higher as compared with the non-loading condition. The loading and displacement were measured at a sampling rate of 20 Hz using MAX™ software (Instron Corp.) in a total of 15,000 cycles (Figure 3B) [45]. Then, we measured the strength against the displacement of the FHI due to the loading stress [46,47]. In each cycle of loading, we measured the degree of the displacement of the FHI through a scatter plotting analysis using a load versus displacement graph [48,49]. In measuring the bond strength, we defined the initial and final phase of

loading as that applied to the specimen in cycles ranging from 1 to 5000 times and 10,000 to 15,000 times, respectively. Thus, we compared differences in changes in the bond strength at the final phase from the initial phase between the two groups, for which we maintained the degree of loading stress consistently throughout the experiment. Therefore, the magnitude of bond strength was solely dependent on the degree of the displacement of the FHI.

2.4. Scanning Electron Microscopy (SEM)

After selecting four pairs of the specimen obtained from the same cadavers in both groups, we prepared cross-sectional samples by pulling the diamond saw across the center of the bone defects on the coronal plane. Thus, we attempted to measure the bond strength at the largest bone defects (Figure 4).

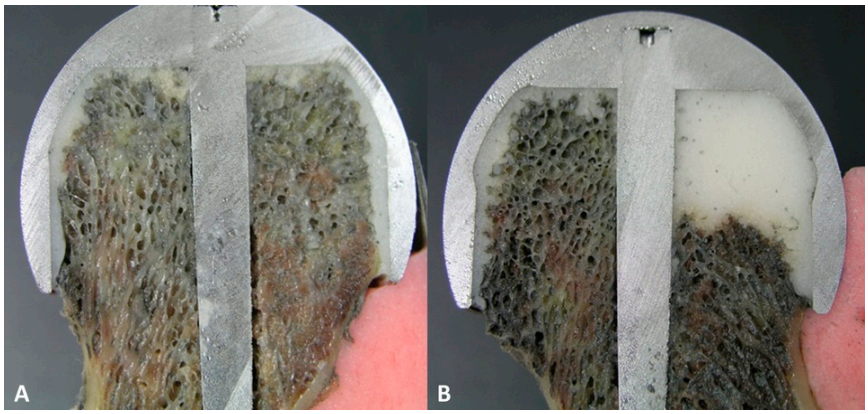

Figure 4. Cross sections of the femoral specimens. (**A**) In the control group, bone cements were used to fill the gap between bone and the implant. There were no other bone defects filled with bone cement. (**B**) In the experimental group, bone defects were used to sufficiently fill 50% of the bone defects. There were no other bone defects.

The samples were completely frozen in a refrigerator (−80 °C) for 24 h and then underwent a freeze-drying process at a temperature of −77 °C for two days. We therefore prepared dry femoral samples. This was followed by SEM to examine the bond strength both at the bone–cement interface and at the implant–cement interface.

2.5. Statistical Analysis

Statistical analysis was carried out using the SPSS version 25.0 (IBM Corp., Armonk, NY, USA). All data were presented as mean ± SD (SD: standard deviation). We compared differences in the size of the FHI and changes in the bond strength at the final phase from the initial phase between the two groups using the Student's *t*-test. A *p*-value of <0.05 was considered statistically significant.

3. Results

3.1. Size of the FHI

The mean size of the FHI was 49.4 ± 2.1 (range, 44–53) mm in the experimental group and 49.1 ± 1.8 (range, 43–52) mm in the control group. However, this difference reached no statistical significance ($p = 0.7356$).

3.2. Results of the Biomechanical Study

Overall, there was an increase in the degree of displacement due to the loading stress with increased loading cycles in both groups. In cycles of up to 6000 times, there was a steep increase. After cycles of 8000 times, however, there was a gradual increase. Moreover, in cycles of up to 8000 times, there was an increase in the difference in the degree of displacement due to the loading stress between the two groups. After cycles of 8000 times, however, such difference remained almost unchanged (Figure 5).

The degree of displacement at each phase is represented in Table 1. Changes in the degree of displacement at the final phase from the initial phase were calculated as 0.089 ± 0.036 mm in the experimental group and 0.083 ± 0.056 mm in the control group. However, this difference reached no statistical significance (p = 0.7789) (Figure 6).

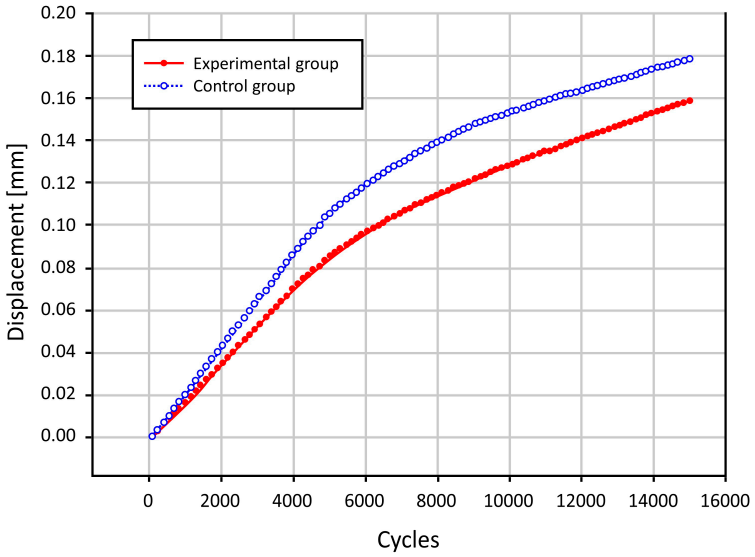

Figure 5. The degree of the displacement of the femoral head implant.

Table 1. The degree of displacement at each phase.

#	Values					
	Experimental Group (n = 10)			Control Group (n = 10)		
	Initial Phase	Final Phase	Δ	Initial Phase	Final Phase	Δ
1	0.237	0.450	0.213	0.051	0.121	0.07
2	0.032	0.066	0.034	0.078	0.190	0.112
3	0.069	0.151	0.082	0.055	0.140	0.085
4	0.031	0.061	0.03	0.109	0.240	0.131
5	0.123	0.251	0.128	0.025	0.073	0.048
6	0.098	0.199	0.01	0.140	0.308	0.168
7	0.042	0.090	0.048	0.075	0.146	0.071
8	0.077	0.172	0.095	0.045	0.104	0.059
9	0.088	0.201	0.113	0.068	0.162	0.094
10	0.062	0.143	0.081	0.052	0.103	0.051

Note: #, specimen identification number; Δ, changes in the degree of displacement at the final phase from the initial phase. All the values are presented at a unit of mm.

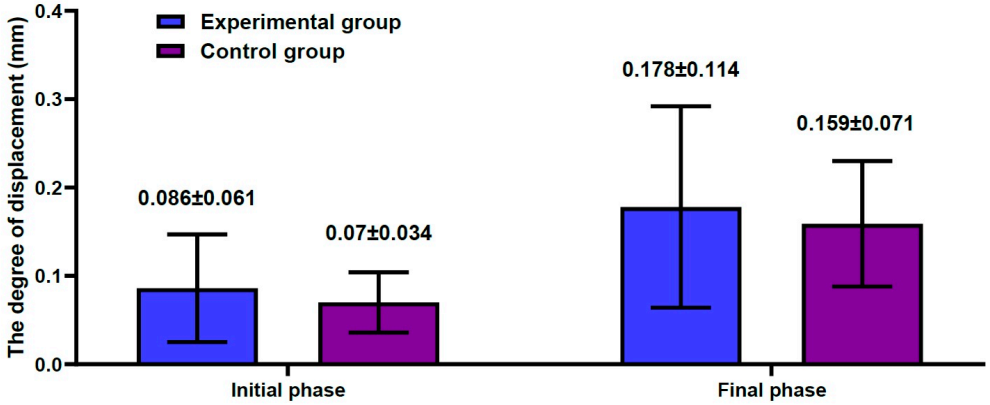

Figure 6. Changes in the degree of displacement at the final phase from the initial phase.

3.3. The Bond Strength at the Bone–Cement Interface

With SEM, all the four pairs of the femoral specimens, obtained from both groups, showed no gap at the bone–cement interface (Figure 7). However, there was a gap of approximately 0.2 mm in size at the interface between the FHI and the bone cement (Figure 8).

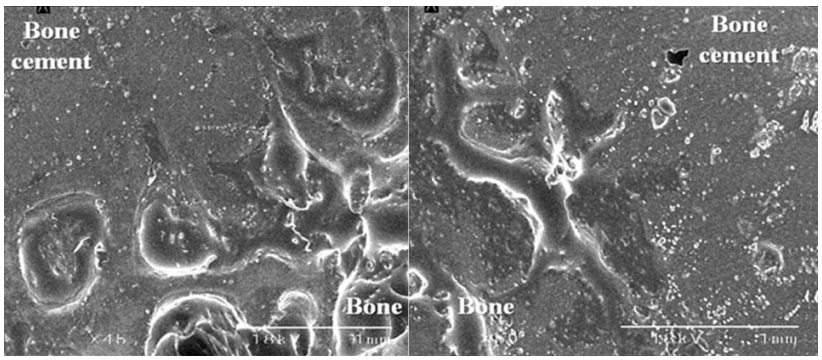

Figure 7. Scanning electron microscopy of the interface between the bone and bone cement. There was no gap between the bone and bone cement in all four pairs of the femoral specimens.

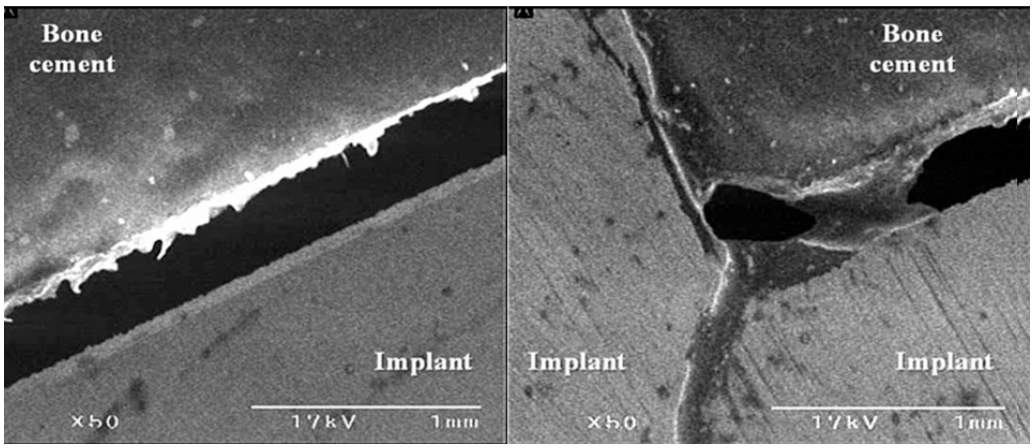

Figure 8. Scanning electron microscopy of the interface between the femoral head implant and bone cement.

4. Discussion

An appropriate experimental model of the human disease is a prerequisite for a clinical trial to assess the efficacy and safety of a novel treatment model in the setting of ONFH [1]. From this context, an animal model of ONFH played a key role in performing a pre-clinical trial to identify more effective treatments, whereas a cellular model was used to clarify the pathogenesis and pathophysiology of ONFH [50]. Nevertheless, many experimental models do not share the same physiological and metabolic characteristics with humans [51,52].

It is mandatory for orthopedic surgeons to obtain a complete understanding of human anatomy; anatomy is a basic medical discipline by which they can achieve improvements in their training. Moreover, cadaveric studies may allow orthopedic surgeons to study the characteristics of many diseases and anatomical structures that are vulnerable to damages, such as bone, muscle and ligament [53].

Cadaveric studies are also useful in performing an assessment of the biomechanics of anatomical structures, thus allowing orthopedic surgeons to develop new surgical techniques [53].

Biomechanical cadaveric studies can be performed when it is not easy to handle the movement or force of interest in the joint or soft tissue in vivo. This enables orthopedic

surgeons to assess biomechanical characteristics and properties. Indeed, biomechanical cadaveric studies play a role in performing a pre-clinical assessment of new surgical techniques and implant designs [54–56]. This justifies the current biomechanical cadaveric study.

Mont MA et al. performed a systematic review of the previous published literature on untreated asymptomatic ONFH, thus showing that >25% involvement of the femoral head served as a risk factor of femoral head collapse [57]. Indeed, the HRA can be performed for patients aged < 50 years old who had necrotic lesions involving <30–33.3% of the femoral head [58,59].

To summarize, our results are as follows: First, changes in the degree of displacement at the final phase from the initial phase were calculated as 0.089 ± 0.036 mm in the experimental group and 0.083 ± 0.056 mm in the control group. However, this difference reached no statistical significance (p = 0.7789). Second, overall there was an increase in the degree of displacement due to the loading stress, with increased loading cycles in both groups. In cycles of up to 6000 times, there was a steep increase. After cycles of 8000 times, however, there was a gradual increase in it. Moreover, in cycles of up to 8000 times there was an increase in the difference in the degree of displacement due to the loading stress between the two groups. After cycles of 8000 times, however, such difference remained almost unchanged. Third, with SEM, all the four pairs of the femoral specimens, obtained from both groups, showed no gap at the bone–cement interface. However, there was a gap of approximately 0.2 mm in size at the interface between the FHI and bone cement.

However, our results cannot be generalized; further studies based on computational modeling are warranted to corroborate them. The necessity of computational modeling of musculoskeletal structures cannot be overlooked; it may be useful in not only providing the data about musculoskeletal structures, but also in simulating injuries and outcomes of surgical operations [60]. Thus, computational modeling and personalized simulations may provide fundamental insights into a better understanding of the pathophysiologic mechanisms underlying injuries. This can contribute to not only reducing the necessity of human or animal experiments, but also enabling orthopedic surgeons to implement novel treatment strategies or to make a plan for surgery [61]. To date, sophisticated approaches to the computational modeling of musculoskeletal structures have emerged. Indeed, such a model has been employed in studies about a specific type of implant or surgical procedure [62]. This is because a meticulous preoperative strategy based on computational modeling is of paramount importance when orthopedic surgeons choose the optimal type of implant [63].

The usefulness of computational modeling in the context of ONFH deserves special attention. It is more advantageous in predicting the whole process without actually performing the surgery as compared with a traditional static analysis [64].

Computational modeling with finite element analysis (FEA) plays a key role in the association with the design and development of a medical device [65]. More specifically, it can be used to assess the deformation field, strain field and stress field of the femoral head and support device [64]. It would, therefore, be worthwhile to explore the value of the FEA in the context of an MoM implant. Of note, the previous literature has simulated a loading by adopting a gait cycle reflecting the actual condition of an implant user [66–70].

An MoM implant is equipped with a higher stability and a lower risk of dislocations. It is harder as compared with ceramic materials; its advantages include a lower rate of fracture failure under high loads and a 20- to 100-fold lower rate of wear as compared with conventional metal-on-polyethylene implants [71]. Due to these benefits, an MoM implant may be used for younger and more active patients [72].

Efforts have been made to decrease the surface contact area (SCA) and to lower the rate of adhesion wear and the coefficient of friction [73]. A dimple is surface texturing that belongs to one such effort made for diverse types of mechanical components; it plays a role in trapping wear debris, preventing the abrasive wear of SCA and generating hydrodynamic pressure to provide additional lift [74,75]. Both theoretical and experimental

studies have shown that surface texturing has a positive effect in improving the tribological performance of a device [76–79].

Jamari J. et al. assessed the effect of dimples on the rate of wear in the context of THA. These authors performed the FEA based on the prediction model with or without dimples. After simulations using 3D physiological loading of the joint under normal walking conditions, Jamari J. et al. showed that the dimples were effective in lowering the contact pressure and wear [80].

To date, orthopedic research has been driven by both biomechanical studies and clinical trials [81–84]. A cadaveric biomechanical study remains a useful method in that it allows surgeons, engineers and researchers to achieve results similar to in vivo clinical studies without endangering patients [53,85]. From this context, the current results are of significance in that this is a pilot experiment using a cadaveric model of the ONFH involving up to 50% of the remaining femoral head in Korea for future clinical studies. However, more efforts should be made to translate the current results into clinical practice.

5. Conclusions

In conclusion, our results indicate that orthopedic surgeons could consider performing the HRA in patients with ONFH where the bone defects involve up to 50% of the remaining femoral head without involving the femoral head–neck junction in the anterior and superior area of the femoral head. However, more evidence-based studies are warranted to justify our results.

Author Contributions: Conceptualization, S.W., Y.L. and D.S.; data curation, S.W. and Y.L.; formal analysis, S.W. and Y.L.; investigation, S.W. and Y.L.; methodology, S.W. and Y.L.; project administration, D.S.; resources, S.W. and Y.L.; supervision, D.S.; visualization, S.W. and Y.L.; writing—original draft, S.W. and Y.L.; writing—review and editing, S.W., Y.L. and D.S. All authors will be informed about each step of manuscript processing, including submission, revision, revision reminder, etc., via emails from the assigned Assistant Editor. All authors have read and agreed to the published version of the manuscript.

Funding: This research received no external funding.

Institutional Review Board Statement: We obtained the ethical approval of the current study from the Internal Institutional Review Board (IRB) of the Korea National Institute of Bioethics Pol-504 icy (IRB approval #: P01-202101-15-019; date of approval: 23 March 2021) and conducted it in compliance with the relevant guidelines and applicable laws. But a written informed consent was waived because this is a cadaveric study.

Informed Consent Statement: Not applicable.

Data Availability Statement: All data generated or analysed during this study are included in this published article.

Conflicts of Interest: The authors declare no conflict of interest.

References

1. Cardín-Pereda, A.; García-Sánchez, D.; Terán-Villagrá, N.; Alfonso-Fernández, A.; Fakkas, M.; Garcés-Zarzalejo, C.; Pérez-Campo, F.M. Osteonecrosis of the Femoral Head: A Multidisciplinary Approach in Diagnostic Accuracy. *Diagnostics* **2022**, *12*, 1731. [CrossRef]
2. Murab, S.; Hawk, T.; Snyder, A.; Herold, S.; Totapally, M.; Whitlock, P.W. Tissue Engineering Strategies for Treating Avascular Necrosis of the Femoral Head. *Bioengineering* **2021**, *8*, 200. [CrossRef]
3. Konarski, W.; Poboży, T.; Śliwczyński, A.; Kotela, I.; Krakowiak, J.; Hordowicz, M.; Kotela, A. Avascular Necrosis of Femoral Head—Overview and Current State of the Art. *Int. J. Environ. Res. Public Health* **2022**, *19*, 7348. [CrossRef] [PubMed]
4. Petek, D.; Hannouche, D.; Suva, D. Osteonecrosis of the femoral head: Pathophysiology and current concepts of treatment. *EFORT Open Rev.* **2019**, *4*, 85–97. [CrossRef]
5. Bejar, J.; Peled, E.; Boss, J.H. Vasculature deprivation-induced osteonecrosis of the rat femoral head as a model for therapeutic trials. *Theor. Biol. Med. Model* **2005**, *2*, 24. [CrossRef]
6. Choi, H.R.; Steinberg, M.E.; Y Cheng, E. Osteonecrosis of the femoral head: Diagnosis and classification systems. *Curr. Rev. Musculoskelet. Med.* **2015**, *8*, 210–220. [CrossRef]

7. Rezus, E.; Tamba, B.I.; Badescu, M.C.; Popescu, D.; Bratoiu, I.; Rezus, C. Osteonecrosis of the Femoral Head in Patients with Hypercoagulability—From Pathophysiology to Therapeutic Implications. *Int. J. Mol. Sci.* **2021**, *22*, 6801. [CrossRef] [PubMed]
8. Fu, D.; Qin, K.; Yang, S.; Lu, J.; Lian, H.; Zhao, D. Proper mechanical stress promotes femoral head recovery from steroid-induced osteonecrosis in rats through the OPG/RANK/RANKL system. *BMC Musculoskelet. Disord.* **2020**, *21*, 281. [CrossRef]
9. Paderno, E.; Zanon, V.; Vezzani, G.; Giacon, T.A.; Bernasek, T.L.; Camporesi, E.M.; Bosco, G. Evidence-Supported HBO Therapy in Femoral Head Necrosis: A Systematic Review and Meta-Analysis. *Int. J. Environ. Res. Public Health* **2021**, *18*, 2888. [CrossRef] [PubMed]
10. Wang, A.; Ren, M.; Wang, J. The pathogenesis of steroid-induced osteonecrosis of the femoral head: A systematic review of the literature. *Gene* **2018**, *671*, 103–109. [CrossRef]
11. Tsai, S.W.; Wu, P.K.; Chen, C.F.; Chiang, C.C.; Huang, C.K.; Chen, T.H.; Liu, C.L.; Chen, W.M. Etiologies and outcome of osteonecrosis of the femoral head: Etiology and outcome study in a Taiwan population. *J. Chin. Med. Assoc.* **2016**, *79*, 39–45. [CrossRef] [PubMed]
12. Kunze, K.N.; Sullivan, S.W.; Nwachukwu, B.U. Updates on Management of Avascular Necrosis Using Hip Arthroscopy for Core Decompression. *Front Surg.* **2022**, *9*, 662722. [CrossRef] [PubMed]
13. Karasuyama, K.; Motomura, G.; Ikemura, S.; Fukushi, J.I.; Hamai, S.; Sonoda, K.; Kubo, Y.; Yamamoto, T.; Nakashima, Y. Risk factor analysis for postoperative complications requiring revision surgery after transtrochanteric rotational osteotomy for osteonecrosis of the femoral head. *J. Orthop. Surg. Res.* **2018**, *13*, 6. [CrossRef] [PubMed]
14. Maruyama, M.; Nabeshima, A.; Pan, C.C.; Behn, A.W.; Thio, T.; Lin, T.; Pajarinen, J.; Kawai, T.; Takagi, M.; Goodman, S.B.; et al. The effects of a functionally-graded scaffold and bone marrow-derived mononuclear cells on steroid-induced femoral head osteonecrosis. *Biomaterials* **2018**, *187*, 39–46. [CrossRef]
15. Bakircioglu, S.; Atilla, B. Hip preserving procedures for osteonecrosis of the femoral head after collapse. *J. Clin. Orthop. Trauma* **2021**, *23*, 101636. [CrossRef]
16. Tripathy, S.K.; Goyal, T.; Sen, R.K. Management of femoral head osteonecrosis: Current concepts. *Indian J. Orthop.* **2015**, *49*, 28–45. [CrossRef]
17. Zhang, Q.Y.; Li, Z.R.; Gao, F.Q.; Sun, W. Pericollapse Stage of Osteonecrosis of the Femoral Head: A Last Chance for Joint Preservation. *Chin. Med. J.* **2018**, *131*, 2589–2598. [CrossRef]
18. Kuroda, Y.; Nankaku, M.; Okuzu, Y.; Kawai, T.; Goto, K.; Matsuda, S. Percutaneous autologous impaction bone graft for advanced femoral head osteonecrosis: A retrospective observational study of unsatisfactory short-term outcomes. *J. Orthop. Surg. Res.* **2021**, *16*, 141. [CrossRef]
19. Jie, K.; Feng, W.; Li, F.; Wu, K.; Chen, J.; Zhou, G.; Zeng, H.; Zeng, Y. Long-term survival and clinical outcomes of non-vascularized autologous and allogeneic fibular grafts are comparable for treating osteonecrosis of the femoral head. *J. Orthop. Surg. Res.* **2021**, *16*, 109. [CrossRef]
20. Ma, J.; Sun, W.; Gao, F.; Guo, W.; Wang, Y.; Li, Z. Porous Tantalum Implant in Treating Osteonecrosis of the Femoral Head: Still a Viable Option? *Sci. Rep.* **2016**, *6*, 28227. [CrossRef]
21. Yang, L.; Boyd, K.; Kaste, S.C.; Kamdem Kamdem, L.; Rahija, R.J.; Relling, M.V. A mouse model for glucocorticoid-induced osteonecrosis: Effect of a steroid holiday. *J. Orthop. Res.* **2009**, *27*, 169–175. [CrossRef]
22. Sugano, N.; Kubo, T.; Takaoka, K.; Ohzono, K.; Hotokebuchi, T.; Matsumoto, T.; Igarashi, H.; Ninomiya, S. Diagnostic criteria for non-traumatic osteonecrosis of the femoral head. A multicentre study. *J. Bone Joint Surg. Br.* **1999**, *81*, 590–595. [CrossRef] [PubMed]
23. Iwakiri, K.; Oda, Y.; Kaneshiro, Y.; Iwaki, H.; Masada, T.; Kobayashi, A.; Asada, A.; Takaoka, K. Effect of simvastatin on steroid-induced osteonecrosis evidenced by the serum lipid level and hepatic cytochrome P4503A in a rabbit model. *J. Orthop. Sci.* **2008**, *13*, 463–468. [CrossRef] [PubMed]
24. Ichiseki, T.; Matsumoto, T.; Nishino, M.; Kaneuji, A.; Katsuda, S. Oxidative stress and vascular permeability in steroid-induced osteonecrosis model. *J. Orthop. Sci.* **2004**, *9*, 509–515. [CrossRef]
25. Yamamoto, T.; Hirano, K.; Tsutsui, H.; Sugioka, Y.; Sueishi, K. Corticosteroid enhances the experimental induction of osteonecrosis in rabbits with Shwartzman reaction. *Clin. Orthop. Relat. Res.* **1995**, *316*, 235–243. [CrossRef]
26. Wu, X.; Yang, S.; Duan, D.; Zhang, Y.; Wang, J. Experimental osteonecrosis induced by a combination of low-dose lipopolysaccharide and high-dose methylprednisolone in rabbits. *Jt. Bone Spine* **2008**, *75*, 573–578. [CrossRef]
27. Qin, L.; Zhang, G.; Sheng, H.; Yeung, K.W.; Yeung, H.Y.; Chan, C.W.; Cheung, W.H.; Griffith, J.; Chiu, K.H.; Leung, K.S. Multiple bioimaging modalities in evaluation of an experimental osteonecrosis induced by a combination of lipopolysaccharide and methylprednisolone. *Bone* **2006**, *39*, 863–871. [CrossRef]
28. Calkins, T.E.; Suleiman, L.I.; Culvern, C.; Alazzawi, S.; Kazarian, G.S.; Barrack, R.L.; Haddad, F.S.; Della Valle, C.J. Hip resurfacing arthroplasty and total hip arthroplasty in the same patient: Which do they prefer? *Hip Int.* **2021**, *31*, 328–334. [CrossRef]
29. Clough, E.J.; Clough, T.M. Metal on metal hip resurfacing arthroplasty: Where are we now? *J. Orthop.* **2020**, *23*, 123–127. [CrossRef]
30. Park, C.W.; Lim, S.J.; Kim, J.H.; Park, Y.S. Hip resurfacing arthroplasty for osteonecrosis of the femoral head: Implant-specific outcomes and risk factors for failure. *J. Orthop. Translat.* **2020**, *21*, 41–48. [CrossRef]
31. Kabata, T.; Maeda, T.; Tanaka, K.; Yoshida, H.; Kajino, Y.; Horii, T.; Yagishita, S.; Tsuchiya, H. Hemi-resurfacing versus total resurfacing for osteonecrosis of the femoral head. *J. Orthop. Surg.* **2011**, *19*, 177–180. [CrossRef]

32. Sodhi, N.; Acuna, A.; Etcheson, J.; Mohamed, N.; Davila, I.; Ehiorobo, J.O.; Jones, L.C.; Delanois, R.E.; Mont, M.A. Management of osteonecrosis of the femoral head. *Bone Jt. J.* **2020**, *102-B*, 122–128. [CrossRef]
33. Ball, S.T.; Le Duff, M.J.; Amstutz, H.C. Early results of conversion of a failed femoral component in hip resurfacing arthroplasty. *J. Bone Joint Surg. Am.* **2007**, *89*, 735–741. [CrossRef] [PubMed]
34. Murray, D.W.; Grammatopoulos, G.; Gundle, R.; Gibbons, C.L.; Whitwell, D.; Taylor, A.; Glyn-Jones, S.; Pandit, H.G.; Ostlere, S.; Gill, H.S.; et al. Hip resurfacing and pseudotumour. *Hip Int.* **2011**, *21*, 279–283. [CrossRef]
35. Tai, C.L.; Chen, Y.C.; Hsieh, P.H. The effects of necrotic lesion size and orientation of the femoral component on stress alterations in the proximal femur in hip resurfacing—A finite element simulation. *BMC Musculoskelet. Disord.* **2014**, *15*, 262. [CrossRef]
36. Su, E.P.; Ho, H.; Bhal, V.; Housman, L.R.; Masonis, J.L.; Noble, J.W., Jr.; Hopper, R.H., Jr.; Engh, C.A., Jr. Results of the First U.S. FDA-Approved Hip Resurfacing Device at 10-Year Follow-up. *J. Bone Joint Surg. Am.* **2021**, *103*, 1303–1311. [CrossRef] [PubMed]
37. Food and Drug Administration. P040033: Birmingham Hip Resurfacing (BHR) System. 2006. Available online: http://www.accessdata.fda.gov/cdrh_docs/pdf4/p040033a.pdf (accessed on 9 February 2023).
38. Gross, T.P.; Liu, F.; Webb, L.A. Clinical outcome of the metal-on-metal hybrid Corin Cormet 2000 hip resurfacing system: An up to 11-year follow-up study. *J. Arthroplast.* **2012**, *27*, 533–538.e1. [CrossRef]
39. Mogensen, S.L.; Jakobsen, T.; Christoffersen, H.; Krarup, N. High Re-Operation Rates Using Conserve Metal-On-Metal Total Hip Articulations. *Open Orthop. J.* **2016**, *10*, 41–48. [CrossRef] [PubMed]
40. Samuel, A.M.; Rathi, V.K.; Grauer, J.N.; Ross, J.S. How do Orthopaedic Devices Change After Their Initial FDA Premarket Approval? *Clin. Orthop. Relat. Res.* **2016**, *474*, 1053–1068. [CrossRef] [PubMed]
41. Waewsawangwong, W.; Ruchiwit, P.; Huddleston, J.I.; Goodman, S.B. Hip arthroplasty for treatment of advanced osteonecrosis: Comprehensive review of implant options, outcomes and complications. *Orthop. Res. Rev.* **2016**, *8*, 13–29.
42. Yamamoto, N.; Sukegawa, S.; Kitamura, A.; Goto, R.; Noda, T.; Nakano, K.; Takabatake, K.; Kawai, H.; Nagatsuka, H.; Kawasaki, K.; et al. Deep Learning for Osteoporosis Classification Using Hip Radiographs and Patient Clinical Covariates. *Biomolecules* **2020**, *10*, 1534. [CrossRef] [PubMed]
43. Gao, S.; Hu, G. Experimental Study on Biaxial Dynamic Compressive Properties of ECC. *Materials* **2021**, *14*, 1257. [CrossRef] [PubMed]
44. Juvonen, T.; Nuutinen, J.P.; Koistinen, A.P.; Kröger, H.; Lappalainen, R. Biomechanical evaluation of bone screw fixation with a novel bone cement. *Biomed. Eng. Online* **2015**, *14*, 74. [CrossRef] [PubMed]
45. Faris, M.A.; Abdullah, M.M.A.B.; Muniandy, R.; Abu Hashim, M.F.; Błoch, K.; Jeż, B.; Garus, S.; Palutkiewicz, P.; Mohd Mortar, N.A.; Ghazali, M.F. Comparison of Hook and Straight Steel Fibers Addition on Malaysian Fly Ash-Based Geopolymer Concrete on the Slump, Density, Water Absorption and Mechanical Properties. *Materials* **2021**, *14*, 1310. [CrossRef]
46. Xu, H.Z.; Wang, X.Y.; Chi, Y.L.; Zhu, Q.A.; Lin, Y.; Huang, Q.S.; Dai, L.Y. Biomechanical evaluation of a dynamic pedicle screw fixation device. *Clin. Biomech.* **2006**, *21*, 330–336. [CrossRef] [PubMed]
47. Nourisa, J.; Rouhi, G. Biomechanical evaluation of intramedullary nail and bone plate for the fixation of distal metaphyseal fractures. *J. Mech. Behav. Biomed. Mater.* **2016**, *56*, 34–44. [CrossRef]
48. Motavalli, M.; Whitney, G.A.; Dennis, J.E.; Mansour, J.M. Investigating a continuous shear strain function for depth-dependent properties of native and tissue engineering cartilage using pixel-size data. *J. Mech. Behav. Biomed. Mater.* **2013**, *28*, 62–70. [CrossRef] [PubMed]
49. Gomez, A.D.; Zou, H.; Shiu, Y.T.; Hsu, E.W. Characterization of regional deformation and material properties of the intact explanted vein by microCT and computational analysis. *Cardiovasc. Eng. Technol.* **2014**, *5*, 359–370. [CrossRef]
50. Li, Z.; Shao, W.; Lv, X.; Wang, B.; Han, L.; Gong, S.; Wang, P.; Feng, Y. Advances in experimental models of osteonecrosis of the femoral head. *J. Orthop. Translat.* **2023**, *39*, 88–99. [CrossRef]
51. Xu, J.; Gong, H.; Lu, S.; Deasey, M.J.; Cui, Q. Animal models of steroid-induced osteonecrosis of the femoral head-a comprehensive research review up to 2018. *Int. Orthop.* **2018**, *42*, 1729–1737. [CrossRef] [PubMed]
52. Zheng, L.Z.; Liu, Z.; Lei, M.; Peng, J.; He, Y.X.; Xie, X.H.; Man, C.W.; Huang, L.; Wang, X.L.; Fong, D.T.; et al. Steroid-associated hip joint collapse in bipedal emus. *PLoS ONE* **2013**, *8*, e76797. [CrossRef] [PubMed]
53. Dal Fabbro, G.; Agostinone, P.; Lucidi, G.A.; Pizza, N.; Maitan, N.; Grassi, A.; Zaffagnini, S. The Cadaveric Studies and the Definition of the Antero-Lateral Ligament of the Knee: From the Anatomical Features to the Patient-Specific Reconstruction Surgical Techniques. *Int. J. Environ. Res. Public Health* **2021**, *18*, 12852. [CrossRef] [PubMed]
54. Kwak, D.-S.; Kim, Y.D.; Cho, N.; In, Y.; Kim, M.S.; Lim, D.; Koh, I.J. Restoration of the Joint Line Configuration Reproduces Native Mid-Flexion Biomechanics after Total Knee Arthroplasty: A Matched-Pair Cadaveric Study. *Bioengineering* **2022**, *9*, 564. [CrossRef] [PubMed]
55. Liu, A.; Sanderson, W.J.; Ingham, E.; Fisher, J.; Jennings, L.M. Development of a specimen-specific in vitro pre-clinical simulation model of the human cadaveric knee with appropriate soft tissue constraints. *PLoS ONE* **2020**, *15*, e0238785. [CrossRef]
56. Vanaclocha, A.; Vanaclocha, V.; Atienza, C.M.; Clavel, P.; Jordá-Gómez, P.; Barrios, C.; Saiz-Sapena, N.; Vanaclocha, L. Bionate Lumbar Disc Nucleus Prosthesis: Biomechanical Studies in Cadaveric Human Spines. *ACS Omega* **2022**, *7*, 46501–46514. [CrossRef] [PubMed]

57. Mont, M.A.; Zywiel, M.G.; Marker, D.R.; McGrath, M.S.; Delanois, R.E. The natural history of untreated asymptomatic osteonecrosis of the femoral head: A systematic literature review. *J. Bone Joint Surg. Am.* **2010**, *92*, 2165–2170. [CrossRef]
58. Kaushik, A.P.; Das, A.; Cui, Q. Osteonecrosis of the femoral head: An update in year 2012. *World J. Orthop.* **2012**, *3*, 49–57. [CrossRef] [PubMed]
59. Della Valle, C.J.; Nunley, R.M.; Raterman, S.J.; Barrack, R.L. Initial American experience with hip resurfacing following FDA approval. *Clin. Orthop. Relat. Res.* **2009**, *467*, 72–78. [CrossRef]
60. Liacouras, P.C.; Wayne, J.S. Computational modeling to predict mechanical function of joints: Application to the lower leg with simulation of two cadaver studies. *J. Biomech. Eng.* **2007**, *129*, 811–817. [CrossRef]
61. Weickenmeier, J.; Butler, C.A.M.; Young, P.G.; Goriely, A.; Kuhl, E. The mechanics of decompressive craniectomy: Personalized simulations. *Comput. Methods Appl. Mech. Eng.* **2017**, *314*, 180–195. [CrossRef]
62. Scifert, C.F.; Noble, P.C.; Brown, T.D.; Bartz, R.L.; Kadakia, N.; Sugano, N.; Johnston, R.C.; Pedersen, D.R.; Callaghan, J.J. Experimental and computational simulation of total hip arthroplasty dislocation. *Orthop. Clin. North Am.* **2001**, *32*, 553–567. [CrossRef] [PubMed]
63. Peng, M.J.; Chen, H.Y.; Hu, Y.; Ju, X.; Bai, B. Finite Element Analysis of porously punched prosthetic short stem virtually designed for simulative uncemented Hip Arthroplasty. *BMC Musculoskelet. Disord.* **2017**, *18*, 295. [CrossRef]
64. Yi, W.; Tian, Q.; Dai, Z.; Liu, X. Mechanical behaviour of umbrella-shaped, Ni-Ti memory alloy femoral head support device during implant operation: A finite element analysis study. *PLoS ONE* **2014**, *9*, e100765. [CrossRef]
65. Goel, V.K.; Nyman, E. Computational Modeling and Finite Element Analysis. *Spine* **2016**, *41* (Suppl. 7), S6–S7. [CrossRef]
66. Ammarullah, M.I.; Santoso, G.; Sugiharto, S.; Supriyono, T.; Wibowo, D.B.; Kurdi, O.; Tauviqirrahman, M.; Jamari, J. Minimizing Risk of Failure from Ceramic-on-Ceramic Total Hip Prosthesis by Selecting Ceramic Materials Based on Tresca Stress. *Sustainability* **2022**, *14*, 13413. [CrossRef]
67. Jamari, J.; Ammarullah, M.I.; Santoso, G.; Sugiharto, S.; Supriyono, T.; van der Heide, E. In Silico Contact Pressure of Metal-on-Metal Total Hip Implant with Different Materials Subjected to Gait Loading. *Metals* **2022**, *12*, 1241. [CrossRef]
68. Ammarullah, M.I.; Afif, I.Y.; Maula, M.I.; Winarni, T.I.; Tauviqirrahman, M.; Akbar, I.; Basri, H.; van der Heide, E.; Jamari, J. Tresca Stress Simulation of Metal-on-Metal Total Hip Arthroplasty during Normal Walking Activity. *Materials* **2021**, *14*, 7554. [CrossRef] [PubMed]
69. Jamari, J.; Ammarullah, M.I.; Santoso, G.; Sugiharto, S.; Supriyono, T.; Prakoso, A.T.; Basri, H.; van der Heide, E. Computational Contact Pressure Prediction of CoCrMo, SS 316L and Ti6Al4V Femoral Head against UHMWPE Acetabular Cup under Gait Cycle. *J. Funct. Biomater.* **2022**, *13*, 64. [CrossRef]
70. Jamari, J.; Ammarullah, M.I.; Santoso, G.; Sugiharto, S.; Supriyono, T.; Permana, M.S.; Winarni, T.I.; van der Heide, E. Adopted walking condition for computational simulation approach on bearing of hip joint prosthesis: Review over the past 30 years. *Heliyon* **2022**, *8*, e12050. [CrossRef]
71. Hu, C.Y.; Yoon, T.R. Recent Updates for Biomaterials Used in Total Hip Arthroplasty. *Biomater. Res.* **2018**, *22*, 33. [CrossRef]
72. Harun, M.N.; Wang, F.C.; Jin, Z.M.; Fisher, J. Long-Term Contact-CoupledWear Prediction for Metal-on-Metal Total Hip Joint Replacement. *Proc. Inst. Mech. Eng. Part J J. Eng. Tribol.* **2009**, *223*, 993–1001. [CrossRef]
73. Choudhury, D.; Lackner, J.; Fleming, R.A.; Goss, J.; Chen, J.; Zou, M. Diamond-like Carbon Coatings with Zirconium-Containing Interlayers for Orthopedic Implants. *J. Mech. Behav. Biomed. Mater.* **2017**, *68*, 51–61. [CrossRef] [PubMed]
74. Basri, H.; Syahrom, A.; Ramadhoni, T.S.; Prakoso, A.T.; Ammarullah, M.I. The Analysis of the Dimple Arrangement of the Artificial Hip Joint to the Performance of Lubrication. *IOP Conf. Ser. Mater. Sci. Eng.* **2019**, *620*, 1–10. [CrossRef]
75. Basri, H.; Syahrom, A.; Prakoso, A.T.; Wicaksono, D.; Amarullah, M.I.; Ramadhoni, T.S.; Nugraha, R.D. The Analysis of Dimple Geometry on Artificial Hip Joint to the Performance of Lubrication. *J. Phys. Conf. Ser.* **2019**, *1198*, 1–10. [CrossRef]
76. Ammarullah, M.I.; Saad, A.P.; Syahrom, A. Contact Pressure Analysis of Acetabular Cup Surface with Dimple Addition on Total Hip Arthroplasty Using Finite Element Method. *IOP Conf. Ser. Mater. Sci. Eng.* **2021**, *1034*, 1–11. [CrossRef]
77. Wang, W.; He, Y.; Li, Y.; Wei, B.; Hu, Y.; Luo, J. Investigation on Inner Flow Field Characteristics of Groove Textures in Fully Lubricated Thrust Bearings. *Ind. Lubr. Tribol.* **2018**, *70*, 754–763. [CrossRef]
78. Pratap, T.; Patra, K. Mechanical Micro-Texturing of Ti-6Al-4V Surfaces for Improved Wettability and Bio-Tribological Performances. *Surf. Coat. Technol.* **2018**, *349*, 71–81. [CrossRef]
79. Choudhury, D.; Vrbka, M.; Bin Mamat, A.; Stavness, I.; Roy, C.K.; Mootanah, R.; Krupka, I. The impact of surface and geometry on coefficient of friction of artificial hip joints. *J. Mech. Behav. Biomed. Mater.* **2017**, *72*, 192–199. [CrossRef]
80. Jamari, J.; Ammarullah, M.I.; Saad, A.P.M.; Syahrom, A.; Uddin, M.; van der Heide, E.; Basri, H. The Effect of Bottom Profile Dimples on the Femoral Head on Wear in Metal-on-Metal Total Hip Arthroplasty. *J. Funct. Biomater.* **2021**, *12*, 38. [CrossRef] [PubMed]
81. Jain, A.K. Research in orthopedics: A necessity. *Indian J. Orthop.* **2009**, *43*, 315–317. [CrossRef] [PubMed]
82. Lu, C.; Buckley, J.M.; Colnot, C.; Marcucio, R.; Miclau, T. Basic research in orthopedic surgery: Current trends and future directions. *Indian J. Orthop.* **2009**, *43*, 318–323. [PubMed]
83. Nayar, S.K.; Dein, E.J.; Bernard, J.A.; Zikria, B.A.; Spiker, A.M. Basic Science Research Trends in Orthopedic Surgery: An Analysis of the Top 100 Cited Articles. *HSS J.* **2018**, *14*, 333–337. [CrossRef] [PubMed]

84. Madry, H.; Grässel, S.; Nöth, U.; Relja, B.; Bernstein, A.; Docheva, D.; Kauther, M.D.; Katthagen, J.C.; Bader, R.; van Griensven, M.; et al. The future of basic science in orthopaedics and traumatology: Cassandra or Prometheus? *Eur. J. Med. Res.* **2021**, *26*, 56. [CrossRef]
85. Maletsky, L.; Shalhoub, S.; Fitzwater, F.; Eboch, W.; Dickinson, M.; Akhbari, B.; Louie, E. In Vitro Experimental Testing of the Human Knee: A Concise Review. *J. Knee Surg.* **2016**, *29*, 138–148. [PubMed]